Communications Biology

https://doi.org/10.1038/s42003-026-09885-4

Article in Press

Rod photoreceptors control the ON vs OFF polarity of cone-signaling neurons

Received: 4 June 2025

Accepted: 6 March 2026

Cite this article as: Beaudoin, D.L., Hassan, A.R., Shehu, A. *et al.* Rod photoreceptors control the ON vs OFF polarity of cone-signaling neurons. *Commun Biol* (2026). https://doi.org/10.1038/s42003-026-09885-4

Deborah Langrill Beaudoin, Abdul Rhman Hassan, Angela Shehu, Jeremy M. Bohl, Yumiko Umino, Eduardo C. Solessio, Seongho Kim, Chase B. Hellmer & Tomomi Ichinose

Rod photoreceptors control the ON vs OFF polarity of cone-signaling neurons

Running title: ON and OFF polarity switch

Authors:

Deborah Langrill Beaudoin[1†], Abdul Rhman Hassan[1†], Angela Shehu[1], Jeremy M. Bohl[1], Yumiko Umino[2], Eduardo C. Solessio[2], Seongho Kim[3,4], Chase B. Hellmer[1], Tomomi Ichinose[1,5*]

[†]: these authors contributed equally

*: corresponding author

[1]Department of Ophthalmology, Visual and Anatomical Sciences,

Wayne State University School of Medicine, Detroit, MI, USA

[2]Department of Ophthalmology,

State University of New York, Upstate Medical University, Syracuse, NY, USA

[3]Department of Oncology,

Wayne State University School of Medicine, Detroit, MI, USA

[4]Biostatistics and Bioinformatics Core, Karmanos Cancer Institute,

Wayne State University School of Medicine, Detroit, MI, USA

[5]Department of Pharmacology,

Wayne State University School of Medicine, Detroit, MI, USA

Corresponding Author:

Tomomi Ichinose, tichinos@med.wayne.edu

Abstract

A fundamental feature of the visual system is its ability to detect image contrast. The contrast processing starts in the first synapse of the retina where parallel pathways are established to compute contrast to bright (ON pathway) and dark (OFF pathway) objects, separately transferred to morphologically identified ON and OFF cells throughout the visual system. Here, we found that response polarity in ON and OFF neurons is not fixed but rather switches dynamically to the opposite polarity. The switch was not observed in rod-knockout mice, indicating that rods generate the polarity switch. We determined that neither horizontal cells nor rod-signaling pathways were responsible for the switch. Instead, we discovered that EAAT5 glutamate transporters located at photoreceptor terminals were required to produce the polarity switch. Our findings exhibit the plasticity of ON-OFF coding in retinal interneurons and their ability to encode contrast across the visual dynamic range.

Main

The retina in the eye is the first component of the visual system, capturing and processing a wide variety of image signaling. Various image features, such as color and motion, are encoded into separate neural networks, consisting of numerous types of retinal neurons and synapses. The retinal excitatory pathway starts from the first-order neurons, the rod and cone photoreceptors. Signals are transferred to second-order neurons, bipolar cells, and then to third-order neurons, ganglion cells. Numerous kinds of image signals are encoded into multiple types of retinal cell types and networks, starting at the first visual synapse. Fifteen types of bipolar cells encode different aspects of image signals separately, such as rod (dim) and cone (bright) signals, chromatic and achromatic signals, and ON/OFF signals.

ON and OFF signaling pathways encode positive (bright) and negative (dark) contrasts, respectively. Approximately half of the inner retinal neurons, bipolar, amacrine, and ganglion cells, are categorized as ON cells, excited (or depolarized) by a light stimulus. In contrast, OFF cells are excited by a dark stimulus or shut off (or hyperpolarize) at the light onset. As the signals are transferred from second to third-order neurons, ON and OFF signaling transmission occurs in the different sublaminae of the inner plexiform layer (IPL) in parallel. This morphological and physiological relation was discovered originally by Famiglietti et al. a half-century ago [1, 2], and has been well agreed upon and supported by subsequent retinal studies [3-8].

We previously conducted patch clamp recordings from ON and OFF cone bipolar cells in mouse retinal slice preparations more than 100 cells [4, 5], and rarely observed violations of the ON/OFF morphological-physiological relations. However, when we recently used wholemount retinal preparations, we unexpectedly observed that many second- and third-order neurons exhibited signal polarity switches. ON-OFF polarity has been well-established, and its violation was reported only in rare cases, including Szikra, et al. [9] and Vlasits, et al. [10]. In the present study, we pursued the mechanisms underlying the visual signaling polarity switch.

Results

We conducted patch clamp recordings from starburst amacrine cells (SACs) in wholemount tissues from Ai9; ChAT-cre mice, in which SACs were labeled with tdTomato. We confirmed the SAC recording by injecting a green fluorescent dye, Alexa 488, through the intracellular pipette and morphological examination, which revealed several symmetric primary dendrites having wavy branches and numerous varicosities in the distal branches (Fig. 1a). Physiologically, the SAC recording was confirmed by transient potassium currents without prominent sodium currents in response to voltage steps (Fig. 1b), consistent with previous reports [11]. We targeted both ON and OFF SACs whose somas reside in the ganglion cell layer and inner nuclear layer, respectively [12]. We recorded light-evoked excitatory postsynaptic potentials (L-EPSPs) in ON SACs and found that a fraction of the cells depolarized at light onset, as is expected for ON SACs (n=24, Fig. 1ci). However, unexpectedly, we observed that many other ON SACs hyperpolarized at the light onset (n=34, Fig. 1cii). Such a hyperpolarizing response is typically observed in OFF cells, but somas of the recorded cells were located in the ganglion cell layer, consistent with an ON SAC type. The resting membrane potentials in correct polarity and polarity switching ON SACs did not reveal significant differences (Fig. 1e, Supplementary Table 1). The polarity switches also occurred in ON SACs in C57 wildtype retina (n=9), demonstrating that the switch was not due to the Ai9; ChAT-cre mutant mouse line, nor due to the fluorescent exposure before recordings. OFF SACs also exhibited both correct polarity L-EPSCs and polarity switches (n=2, hyperpolarized; n=8, depolarized Fig. 1d).

ON and OFF polarity switches in SACs were reported previously [13], where the authors observed that the light response polarity switch occurs after light adaptation during the recording as a result of rod photoreceptor bleaching. However, in our recordings, the polarity switch occurred randomly and was not driven by prior light adaptation in mesopic conditions that would have bleached rod photoreceptor pigments (Fig. 1f): approximately half of ON SACs exhibited an ON response, and others showed an OFF response at the beginning of recordings. After approximately 10 minutes of recording, some ON SACs switched from ON to OFF or OFF to ON, while others remained either ON or OFF during the entire recording (Fig. 1f). Potentially, the previous findings [13] revealed the same core event but under different background regimes. However, we decided to investigate further to elucidate the source of the ON and OFF polarity switches. For Fig. 1 and the following dataset, the statistical analysis methods, p-values, and number of cells are summarized in Supplementary Table 1.

The polarity switch was not induced by antagonistic surround, nor by OFF signaling crossover

We first examined whether the unexpected polarity changes were generated by the antagonistic surround mediated through amacrine cells. Amacrine cells release either GABA or glycine to inhibit neurons in the IPL, and ON SACs express both GABA-A and glycine receptors [14-16]. Accordingly, we pursued a pharmacologic approach by applying GABA and glycine receptor antagonists when we encountered ON-SACs with a stable polarity switch. We recorded from a hyperpolarizing ON SAC and found that application of the glycine and GABA-A receptor blockers, strychnine (1 µM) and bicuculline (50 µM), increased the spontaneous activity, but did not change the polarity switch. The cell continued to hyperpolarize in response to light (Fig. 2a). SACs also express GABA-B receptors [17]. However, a GABA-B receptor antagonist, CGP-52432 (10 µM), did not affect the polarity switch (Fig. 2b). We also tested the effects of blocking GABA-

C receptors using TPMPA (50 µM). GABA-C receptors are not expressed by SACs but by presynaptic bipolar cells [18]. Application of a cocktail of GABA and glycine receptor antagonists (bicuculline, CGP52432, TPMPA, strychnine) induced spontaneous activity but had no effects on the polarity switch (Fig. 2c). Altogether, these results indicate that the antagonistic surround did not induce the ON SAC polarity switch.

We then examined whether an OFF signaling crossover induced the polarity switch in ON SACs. We used an mGluR6 agonist, L-AP4 (10 µM), which blocks synaptic transmission from photoreceptors to ON bipolar cells, blocking signaling exclusively in the ON pathway [19]. The application of L-AP4 abolished the hyperpolarizing light response in ON SACs (Fig. 2d), indicating that the polarity switches in ON SACs are induced by ON pathway signaling.

The polarity switch we observed hyperpolarized ON SACs to near -70 mV. We examined whether potassium channels played a role in the hyperpolarizing response because the equilibrium potential of potassium channels is near -86 mV based on the composition of our extracellular and intracellular solutions. SACs express Kv3 channels, a type of voltage-gated potassium channel, near the soma [11]. We applied TEA (1 mM) in the bath solution to block the Kv3 channels, which generated massive spontaneous activity, but the polarity switch remained (Supplementary Fig. 1a). We also applied TEA (10 mM) in the recording pipette to block the channel intracellularly, but this did not affect the polarity switch (Supplementary Fig. 1b). We furthermore tested a cesium intracellular solution to block a broad spectrum of potassium channels, and this also failed to remove the polarity switch (n=9 SACs, Supplementary Fig. 1d). These data indicate that voltage-gated potassium channels did not cause the polarity switch in ON SACs.

Rod-cone interaction induced a polarity switch in ON SACs

Szikra, et al. [9] reported that rods receive cone input through horizontal cells in the mesopic to photopic conditions, inducing the polarity switch in a rod-signaling pathway. Therefore, we examined whether rod-cone interaction induced the polarity switch. When L-EPSPs from ON SACs exhibited a polarity switch in mesopic light conditions, we changed the ambient light conditions from mesopic to photopic. To our surprise, ON-SACs exhibiting the polarity switch in mesopic conditions gradually corrected the polarity as the light levels increased to photopic ranges (Fig. 3a). We also recorded L-EPSPs from OFF SACs whose somas reside in the inner nuclear layer (INL). OFF SACs similarly exhibited a polarity switch: depolarizing at mesopic backgrounds but hyperpolarizing in photopic conditions (Fig. 3b). Furthermore, we recorded from a set of ON SACs in scotopic conditions, which did not show polarity switch (n=10 SACs, Supplementary Fig. 1e). These results suggest that rod and cone interactions in the mesopic light conditions caused the polarity switch.

We tested whether horizontal cells mediated the rod-cone interactions. Horizontal cells' output to cones involves pH change of the photoreceptor synapse, which can be suppressed by applying the pH buffer, HEPES, in the bath solution [20]. HEPES slightly changed the amplitude of the light response; however, the polarity switch was not corrected (Supplementary Fig. 1c,d). Although HEPES did not affect the polarity switch in ON SACs, we examined horizontal cells' contribution using different methods in later experiments.

ON and OFF cone bipolar cells exhibited polarity switch

If rod-cone interaction induced the polarity switch in ON SACs, upstream neurons, bipolar cells, should also show a polarity switch. Our laboratory previously conducted patch clamp recordings from more than 100 ON and OFF cone bipolar cells (CBCs) in slice preparations (250 μm thick), in which ON CBCs, defined by the axon terminals ramifying in the IPL ON sub-laminae, depolarize to light onset, whereas morphologically OFF CBCs hyperpolarize to light onset [4, 5]. We rarely observed violations of the ON and OFF polarities and morphological types, consistent with the fundamental rule in the field [1, 2]. Therefore, we were initially skeptical about ON and OFF polarity switches in CBCs.

Unlike our previous experiments working in retinal slice preparations, here we recorded from bipolar cells using wholemount retinal preparations, the same preparations we used for SAC recordings. We previously established this difficult approach for bipolar cell patch clamp and imaging in wholemount preparations [21, 22]. In mesopic conditions, we observed that many ON CBCs hyperpolarized to light onset, exhibiting a polarity switch (Fig. 3c). Similar to ON SACs, light-evoked hyperpolarization in mesopic conditions was converted to depolarization as the light level increased to the photopic range (Fig. 3c). Similarly, OFF CBCs showed a polarity switch in mesopic conditions, which was changed to the correct polarity in photopic conditions (Fig. 3d). Approximately half of ON and OFF CBCs exhibited polarity switch without clear type-dependency (Table 1, WT). The polarity switch was not associated with changes in the resting membrane potential (Fig. 3e). We occasionally observed polarity switch occurring in an opposite way, correct polarity in mesopic and switched in photopic conditions (Supplementary Fig. 2a). Interestingly, rod bipolar cells did not show a polarity switch but responded both in mesopic and photopic conditions (Supplementary Fig. 2b). Our previous and current data suggest that the polarity switch in bipolar cells was induced by a mechanism only in wholemount preparations, such as lateral circuitry. Because wholemount preparations are more physiological than the slice, we postulate that the polarity switch is a physiological event.

Rod and cone mutant mice and CBC polarity switch

Our data suggest that a rod-cone interaction induced polarity switches in ON and OFF CBCs and SACs (Fig. 3). We used rod or cone functional knockout mice to test the mechanisms of the polarity switch. We first used the *Gnat1*$^{-/-}$ mice in which rods are dysfunctional [23, 24]. Recordings in these mice revealed that ON and OFF CBCs did not respond to light in mesopic conditions (Fig. 4). In photopic conditions, ON CBCs depolarized to light, and OFF CBCs hyperpolarized to light onset, exhibiting no signs of a polarity switch (Fig. 4a). These results suggest that rod photoreceptors induced the polarity switch.

Next, we used the *Cnga3*$^{-/-}$ mice in which cones are dysfunctional, but rods are intact [25, 26]. In mesopic conditions, ON CBCs hyperpolarized at light onset, showing a polarity switch (Fig. 4b, Table 1), additional evidence that rods play a critical role in the polarity switch (Fig. 4a). Then, we tested the photopic condition. Because these mice did not possess functional cones, we expected either the polarity switch to remain, or not to respond to light due to rod bleaching. However, in photopic conditions, the same ON CBCs depolarized, which is the correct polarity for those cells. The polarity switching response occurred again when the light level was decreased to mesopic conditions after the tissue was exposed to bright light conditions

(Supplementary Fig. 3). Correspondingly, OFF CBCs depolarized in the mesopic and hyperpolarized in the photopic conditions (Fig. 4b). More than half of the ON and OFF CBCs we recorded exhibited a polarity switch (Table 1, *Cnga3*$^{-/-}$).

We wondered whether the unexpected photopic response in *Cnga3*$^{-/-}$ mice occurred due to any strain conditions other than cone functional-knockout. We used another cone-dysfunctional mouse strain, *Gnat2*$^{-/-}$ mice [27] to examine if the unexpected photopic response still occurs in CBCs. In the mesopic condition, ON CBCs hyperpolarized and OFF CBCs depolarized, exhibiting a polarity switch, while their photopic responses displayed correct polarity (Fig. 4c & Table 1, *Gnat2*$^{-/-}$). These results confirmed that rods generate both the polarity switch and the correct polarity signals.

The polarity changes occurred within a few minutes after being adapted to a new ambient light level (Supplementary Fig. 3). A short adaptation was required from mesopic to photopic, and photopic to mesopic when repeated (Supplementary Fig. 3). Furthermore, the short adaptation was required for ON and OFF CBCs in wildtype, *Cnga3*$^{-/-}$, and *Gnat2*$^{-/-}$ mice. These results suggest that the polarity switch and correct polarity signals originated in rods but are evoked by different light levels and mediated through different mechanisms.

Gap junctions mediate the correct polarity but not the polarity switch

Rod-cone interactions might occur through rod-cone coupling [28]. We used a gap junction blocker, MFA (50 µM or 100 µM), to examine whether the rod-cone coupling mediated the polarity switch signals. Fig. 5a shows a representative OFF CBC, exhibiting a polarity switch in the mesopic and a correct polarity in the photopic conditions (Fig. 5a, Initial). We applied MFA to observe light responses over 35 minutes in both light conditions. After 5 minutes, the polarity switch in the mesopic conditions did not change, but the hyperpolarizing response (correct polarity) in bright light was reduced. Over 35 minutes of recording, the polarity switch in the mesopic condition stayed the same, while the hyperpolarization (correct polarity) in the photopic condition changed to depolarization (Fig. 5a). The correct polarity became a polarity switch in photopic condition after MFA application. A similar trend was observed in 3 ON and 4 OFF CBCs (Fig. 5b).

Because gap junction blockers might have non-specific effects, we used an additional method to verify the MFA effects. We recorded light-evoked responses in ON and OFF CBCs in *Cx36-fl/fl*; Rho-cre mouse retinas, in which rod-cone coupling was genetically knocked out [29]. In those mice, polarity switches still existed in mesopic conditions. In contrast, in photopic conditions, mixed polarity responses were observed (Correct polarity; 1 ON CBC & 2 OFF CBCs, polarity switch: 3 ON CBCs Fig. 5c-d).

These results suggest the following: (1) The polarity switch and correct polarity signals are mediated to CBCs through distinct pathways. The polarity switch signals were not mediated through gap junctions. (2) The correct polarity signals in photopic conditions were mediated through gap junctions, shown by MFA suppression. The gap-junction blockade revealed that there was a masked polarity switch signal (Fig. 5a). (3) The *Cx36-fl/fl;Rho-Cre* results indicate that rod-cone coupling partially contributed to correct polarity signals in photopic conditions. Cone to CBC transmission and other gap junctions, including between horizontal cells, also

contribute to generating correct polarity in CBCs [30, 31]. We looked further into the contributions of horizontal cells to the polarity switch.

Horizontal cells and mGluR6 contributions to the polarity switch

Only one type of horizontal cell is reported in the mouse retina, which contacts cones with dendritic arbors and rods with their axon terminals [32]. Cellular mechanisms of feedback (from horizontal to photoreceptors) and feedforward (horizontal to bipolar cells) signal transmission are not fully elucidated [33-37]. Furthermore, positive and negative feedback occurs locally and globally from horizontal cells [38], suggesting that complicated modulatory effects occur in the OPL.

Nevertheless, we manipulated the horizontal cell activity by blocking photoreceptor synaptic input with NBQX (10 µM), a potent AMPA receptor antagonist, which was used previously for the photoreceptor-horizontal cell transmission blockade [9]. A representative ON CBC exhibited a polarity switch at the mesopic and a correct polarity in the photopic conditions (Fig. 6a). NBQX had no effect on polarity switched signals in mesopic conditions but changed the correct polarity to a polarity switch in photopic conditions (Fig. 6a). Three out of four ON CBCs and two out of two OFF CBCs exhibited similar results (Fig. 6a, *left*). These results indicate that horizontal cells mediated the correct polarity signals but did not mediate the polarity switch.

We further tested this in *Gnat2*$^{-/-}$ mice in which CBC signals originated solely from rods using an AMPA/kainate glutamate receptor antagonist, CNQX (15 µM) [39, 40]. In these mice, ON CBCs exhibited a polarity switch at the mesopic and a correct polarity in the photopic conditions (Fig. 6b, Fig. 4c). The application of CNQX did not change the polarity switch in the mesopic condition. In contrast, the correct polarity in photopic conditions was converted to a polarity switch by CNQX, depolarizing to light (Fig. 6b, n=8). Some types of OFF CBCs express glutamate receptors sensitive to CNQX [5], and CNQX abolished EPSPs of both polarity switch and correct polarity (n=4)[5]. However, L-EPSPs in other OFF CBCs remained in the presence of CNQX, and exhibited a similar trend: CNQX preserved a polarity switch in mesopic conditions and converted to a polarity switch in photopic conditions (n=4, Fig. 6b). A similar CNQX effect was observed in WT mice, which possess both rods and cones; no changes for the polarity switch in mesopic, but CNQX converted the correct polarity in photopic conditions to a polarity switch (Fig. 6c). All these results with ionotropic glutamate receptor antagonists and HEPES (Fig. 6 & Supplementary Fig. 1c-d) indicate that horizontal cells do not mediate polarity switch signals, but correct polarity signals.

We then tested whether the polarity switching signals were mediated through glutamate receptors on bipolar cell dendrites. We used L-AP4 to block mGluR6-signaling in ON CBCs. L-AP4 abolished both EPSPs with a polarity switch and correct polarity, while both correct polarity signals and inverted polarity signals in OFF CBCs were unaffected by L-AP4 (Supplementary Fig. 4). The results are consistent with the L-AP4 application to SACs (Fig. 2d). Because OFF CBCs express multiple types of glutamate receptors, including kainite and AMPA receptors [5, 41], we could not assess exclusively OFF CBC input. In spite of this limitation, the L-AP4 results confirmed that both polarity switch and non-switch signals were mediated via glutamate receptors on CBC dendrites.

Photoreceptor contributions

In order to assess the polarity of cone photoreceptors, we attempted to record from cones directly. However due to the dominance of rods and the technical difficulty of patching in wholemount retina, we instead recorded from CBCs in voltage-clamp mode. Similar to the recordings in current-clamp mode (Figure 3c-d), both ON and OFF CBCs exhibited a polarity switch: in mesopic conditions, outward currents were observed in ON CBCs, whereas inward currents were observed in OFF CBCs in response to light stimuli. In photopic conditions, CBCs presented the expected response (n= 4 ON CBCs, Supplementary Fig. 4c). These results suggest that cones depolarize in response to a step light stimulation in mesopic conditions.

What can cause light-evoked depolarization in cones? Rod and cone axon terminals express glutamate transporters, EAAT2 and EAAT5, to uptake glutamate released at the terminals [42, 43]. EAAT5 has a large chloride conductance in conjunction with glutamate uptake, which could generate the inhibitory signals [44-47]. We used a glutamate transporter inhibitor, DL-TBOA (50 μM) to test whether EAAT5 generated the polarity switch. ON and OFF CBCs exhibited different polarities of L-EPSPs in mesopic and photopic conditions in wildtype mice (Fig. 7). DL-TBOA corrected the polarity switch (Fig. 7aii, n=6 CBCs, p=0.0006) without affecting the correct polarity signals (Fig. 7bii, n=6 CBCs, p=0.1458). During the DL-TBOA application, the CBC membrane potential was not changed (n=12 CBCs, Fig. 7c), suggesting that EAAT5 resided presynaptic to CBCs. These results suggest that EAAT5 and associated chloride conductance in cone terminals generate depolarizing light responses and induce the polarity switching signals in second-order neurons (Fig. 7d).

Discussion

ON and OFF signals are generated at the first synapse of the retina between photoreceptors and bipolar cells. In the dark, photoreceptors are depolarized and continuously release glutamate. OFF bipolar cells receive glutamatergic inputs through AMPA and kainate glutamate receptors [5, 41, 48], and are depolarized in the dark. In contrast, ON bipolar cells express mGluR6 linking to TrpM1 channels [49-51], and are hyperpolarized in the dark but depolarized in the light as photoreceptor glutamate release is reduced. The ON and OFF dichotomy is separately transferred to ON and OFF sublaminae in the IPL, mediating the signals to ON and OFF amacrine and ganglion cells. This morphological and physiological relation is acknowledged as one of the fundamental rules in retinal neurophysiology [1-3, 7, 8, 52, 53], throughout the visual system [54], and over the ranges of light conditions from scotopic to photopic [55, 56]. Despite the long-established consensus, we found that ON-OFF polarity switch occurs in retinal inner neurons.

There are only a few cases to date where this rule has been shown to be violated. Vlasits, et al. [13] reported that a polarity switch occurs in ON and OFF SACs. This switch even causes directional preference changes in direction-selective ganglion cells (DSGCs) [57, 58]. Furthermore, Szikra, et al. [9] reported that rod photoreceptors exhibit polarity switching signals at high light, which is mediated by cone signaling through horizontal cells. For both cases, the authors found that antagonistic surround through amacrine or horizontal cells was part of the underlying mechanisms. However, we used a relatively small spot of light to evoke light responses, and antagonistic surround was not the reason for the polarity switch (Figs. 2,6 and Supplementary Fig. 1).

A robust polarity switch occurred both in ON and OFF SACs as well as ON and OFF CBCs (Fig. 3). Polarity switch signals were evoked in mesopic, and correct polarity signals were in photopic conditions, suggesting that rod-cone interaction induced the polarity switch. Because the polarity switching occurred within a few minutes (Supplementary Fig. 3) and the pharmacological applications differentially blocked L-EPSPs (Figs. 5,6,7), we showed that two types of signals with opposite polarities were mediated through different mechanisms (Fig. 7c). Although the mechanisms are different, rods generate both polarities of signals (Fig. 4), and glutamate receptors on bipolar cell dendrites mediated both polarities (Supplementary Fig. 4).

Correct polarity L-EPSPs were generated both by cones and rods. L-EPSPs generated by cones were transferred to CBCs and SACs, as shown in photopic conditions, and in the rod-dysfunctional (*Gnat1*$^{-/-}$*-KO*) mice (Figs. 3-4). Rods also evoked correct polarity L-EPSPs in CBCs, as shown by cone-dysfunctional (*Cnga3*$^{-/-}$*-KO* & *Gnat2*$^{-/-}$*-KO*) mice (Fig. 3), as well as in ON-SACs when recorded under scotopic conditions. We expected the involvement of the rod-signaling pathways. Three rod-signaling pathways have been reported, in which gap junctions mediate the primary and secondary pathways from rods to ON and OFF CBCs through AII amacrine-ON CBC and rod-cone coupling, respectively [59]. Our data with MFA revealed that the correct polarity signals were mediated through gap junctions, suggesting the rod-signaling pathway contributions (Fig. 5a-b). L-EPSPs in photopic conditions in *Cx36-fl/fl*;*Rho-cre* mice (rod-cone coupling knockout, Fig. 5c-d) were partially converted to a polarity switch, suggesting that the correct sign signals were mediated through rod-cone coupling to some degree. Along with the results with NBQX/CNQX (Fig. 6), the correct polarity L-EPSPs in CBCs from rods were mediated through three potential pathways: (1) horizontal cells through homocellular gap junctions, (2) rod-cone coupling, and (3) cone to CBC transmission. The L-EPSP polarity in

photopic conditions is the combination of these three inputs plus polarity switching signals. Furthermore, because polarity switches occurred both in ON and OFF CBCs, the contributions of the primary rod-pathway, involving only ON CBCs, and the tertiary pathway, involving only OFF CBCs, were probably not significant. Taken together, these results illustrate that signal polarity across retinal circuits is a fluid property resulting from the interaction of multiple competing mechanisms at the first visual synapse.

Mutant mouse experiments revealed that rods generate the polarity switch signals (Fig. 4), which reach the CBCs through glutamate receptors on their dendrites (Fig. 2d and Supplementary Fig. 3). However, against our expectations, horizontal cells did not produce the polarity switch (Supplementary Fig. 1 & Fig. 6), nor did gap junctions, including rod-cone coupling (Fig. 5). There is a direct synapse between rods and OFF CBCs, but not with ON CBCs [59, 60], which cannot explain the polarity switch in ON CBCs. Without any other putative mechanisms between rods and CBCs to mediate polarity switch signals, we decided to test whether glutamate transporters in photoreceptor terminals contributed to the signals. We found that application of the EAAT transporter blocker, DL-TBOA, removed the polarity switch without affecting correct polarity EPSPs (Fig. 7).

Glutamate transporters, EAAT2 and EAAT5, are expressed by axon terminals of rods and cones [42, 61]. Among those, EAAT5 has a large chloride conductance [47], which might affect the photoreceptor membrane potential and glutamate release. A potential explanation for the results with DL-TBOA is as follows: in dim-light conditions, glutamate is continuously released from rods and cones, inducing the glutamate spillover from those. This activates EAAT5 and the chloride current in cone terminals, inhibiting cones. When a light stimulus reduces the glutamate release from rods, EAAT5-linked chloride conductance is reduced, disinhibiting cones. This results in light-evoked cone depolarization and evoking the polarity switch signal in CBCs.

There are two critical points for this scenario to occur: (1) the spillover occurs among rods and cones and (2) the chloride conductance induces inhibitory currents in cones. Although a massive EAAT5 exists at the rod terminals to clean up released glutamate [44], EAAT5 saturates quickly, and spillover occurs, at least among cones [62, 63]. Rod-to-cone glutamate spillover may also occur. For the second point, previous studies have measured the resting membrane potentials (RMP) as well as the chloride reversal potential (E_{Cl}). The RMP in cones in the mouse retina is between -45 and -55 mV [64], and the E_{Cl} has been reported in various species with a range of values: -42 to -55 mV [65]. These potentials are close to each other, which may not induce any currents. However, photoreceptors are depolarized in dim conditions and may hyperpolarize upon EAAT5-chloride conductance activation.

DL-TBOA-sensitive EAATs on BC dendrites have been reported in the fish [66] and the mouse [67] retinas. If these EAATs generate chloride currents, they are potentially involved in producing a polarity switch. However, DL-TBOA did not change the membrane potentials in our recordings (Results section, Fig. 7). Furthermore, the polarity switch occurred differently in ON and OFF CBCs (Fig. 3), which cannot be induced by EAAT-induced chloride currents if they existed in postsynaptic sites. For these reasons, DL-TBOA-sensitive EAATs were located presynaptically as reported earlier (Fig. 7d) [42, 61].

In our recordings, the polarity switch occurred only in approximately half of CBCs and SACs (Fig. 1, Table 1). This occurred both in ON and OFF cells, but we did not see cell type-dependency, nor retinal topographic distributions. We consider this might be due to the close

proximity of the RMP and E_{Cl}, resulting in a range of EAAT5-Cl^- channel effects on cone membrane potentials across the retina. Our recordings revealed that the CBC polarity switch occurred more frequently in cone-KO than in WT mice (Table 1: *Cnga3*$^{-/-}$: 77%, *Gnat2*$^{-/-}$: 86%, *WT*: 52%). Cones in cone-KO mice do not change the RMP as the ambient light level changes. In contrast, cones in WT mice are hyperpolarized in bright conditions, diminishing the EAAT5-induced hyperpolarization and reducing the occurrence of CBC polarity switch.

Unlike previous studies with slice recordings [4, 5], here we found that more than half of CBCs exhibited a polarity switch (Table 1). We consider that the reason for the difference is the preparation: slice (previous) and wholemount (current) preparations. Wholemount preparations are more physiological than slice preparations, containing intact vertical and lateral neural connections. Interestingly, they preserve not only large neurons, such as horizontal cells, but also rod signaling. Rod photoreceptors saturate their responses at high mesopic conditions: ~10^4 photons/μm^2/s [68, 69]. However, a couple of articles which used wholemount retinal preparations, claim that rods do not saturate [70-72]. In our previous study with slice preparations, we did not observe any light responses in rod bipolar cells when we applied the background light at the “rod-saturating” light level [4]. In contrast, rod-activated responses are evoked from mesopic to photopic conditions in *Cnga3*$^{-/-}$ and *Gnat2*$^{-/-}$ mice (Fig. 4), and rod bipolar cells exhibited light responses in both mesopic and photopic conditions (Supplementary Fig. 2). There might be chemical mechanisms to support rod signaling from the response saturation in *ex vivo* preparations. Presumably, well-preserved rods generate a polarity switch to provide an impact on cone-signaling in mesopic and even up to photopic ranges.

The polarity switch is potentially critical to suppress signals in CBCs and SACs in dim light conditions when rod-signaling is dominant. It may also increase L-EPSPs during the transition from mesopic to photopic conditions by increasing the driving force. Furthermore, instantaneous polarity switching with short adaptation may be critical for the saccadic shift or the continuously moving image of the natural scene. Future research will require clarifying the significance of the ON and OFF polarity switches in retinal neurons.

Methods

Ethical approval

All conducted animal studies adhered to ethical protocols approved by their Institutional Animal Care and Use Committee at Wayne State University (protocol no. 23-11-6310). Experiments were in line with the ARVO Statement for the Use of Animals in Ophthalmic and Visual Research. All procedures were taken to minimize animal suffering and maintain the physiological conditions of the retinal tissues.

Retinal preparation

The experimental techniques used were described in detail in our previous studies [4, 21]. Briefly, both male and female mice, aged 4 – 12 weeks, were used including the C57BL/6J strain (RRID: IMSR_JAX:000664), Ai9 (RCL-tdT) (RRID: IMSR_JAX:007909), R26R-EYFP (RRID: IMSR_JAX: 006148), Chat-cre (RRID: IMSR_JAX: 031661), and Rho-cre (RRID: IMSR_JAX:032909); Jackson Laboratory, Bar Harbor, ME, USA In addition, rod knockout mice (*Gnat1*$^{-/-}$ [73]) and cone knockout mice (*Cnga3*$^{-/-}$) both gifted by Dr. Samar Hattar, cone knockout mice (*Gnat2*$^{-/-}$ [27] gifted by Dr. Marie Burns), and *Cx36-fl/fl* [74] (gifted by Dr. Ribelayga) were also used. All mice were dark adapted overnight before being euthanized using carbon dioxide followed by cervical dislocation and eye enucleation. Retinal tissues were isolated under a stereo microscope. All steps were conducted in dark-adapted conditions utilizing infrared viewers. The dissecting solution was maintained at a cool temperature and continuously oxygenated. The dissections were performed in a HEPES-buffered medium (see solutions section for more details), and the retinal tissues were kept in an oxygenated dark box at room temperature.

Whole-cell recordings

We performed whole-cell patch clamp recordings from bipolar cells and SAC somas in wholemount retinal preparations using an upright microscope (Slicescope Pro 2000, Scientifica, UK) with a CCD camera (Retiga-2000R, Q-Imaging, Canada). The tissues were stabilized with a platinum horseshoe net and nylon wires. The light-evoked postsynaptic potentials and currents (L-EPSPs and L-EPSCs) were recorded at the resting membrane potential and at the equilibrium potential for chloride ions (E_{Cl}; −55 mV), respectively. Recordings were conducted at temperatures between 32-34°C, and liquid junction potentials (~7.4mV) were adjusted post-recording. Electrodes were made from borosilicate glass (1B150F-4; WPI, FL, USA) using a P1000 Puller (Sutter Instruments, CA, USA), with resistances ranging from 6 to 12 MΩ. Clampex and MultiClamp 700B (Molecular Devices, CA, USA) were utilized to generate waveforms, acquire data, and control an LED light stimuli (Cool LED, UK). Data was digitized with an Axon Digidata 1550B (Molecular Devices), filtered at 1 kHz using the four-pole Bessel filter on the MultiClamp 700B, and sampled at rates between 2 and 5 kHz.

Solutions and Drugs

Retinal dissections were carried out in a HEPES-buffered extracellular solution containing 115 mM NaCl, 2.5 mM KCl, 2.5 mM $CaCl_2$, 1.0 mM $MgCl_2$, 10 mM HEPES, and 28 mM glucose, adjusted to a pH of 7.37 using NaOH. Physiological recordings were conducted in Ames' medium, which was buffered with $NaHCO_3$ (Millipore-Sigma, St. Louis, MO, USA) and aerated with 95% O2 and 5% CO_2, maintaining a pH of 7.4 at a temperature range of 30-33°C. The intracellular solution used included 110 mM $KMeSO_3$, 1.0 mM $MgCl_2$, 10.0 mM HEPES, 4.0 mM EGTA, 5.0 mM NaCl, 5.0 mM KCl, 4 mM ATP-Mg, and 0.5 mM GTP-Mg, adjusted to a pH of 7.2 using KOH. We substituted $KMeSO_3$ with $CsMeSO_3$ for the recording in voltage-clamp mode.

The following pharmacological agents were bath applied: a glycine receptor antagonist, strychnine (1 µM, Sigma, St. Louis, MO), a $GABA_A$ receptor antagonist, bicuculline methobromide (50 µM, Enzo Life Sciences, Farmingdale, NY), a $GABA_B$ receptor antagonist CGP-52432 (10 µM, Tocris, Minneapolis, MN), and a $GABA_C$ receptor antagonist, (1,2,5,6-tetrahydropyridin-4-yl) methylphosphinic acid hydrate (TPMPA, 50 µM, Tocris). L-(+)-2-Amino-4-phosphonobutyric acid (L-AP4, 10 µM, Tocris) was used as an mGluR6 agonist. To suppress Kv3 channel activity, 1 mM tetraethylammonium (TEA, Sigma) was bath applied or 10 mM TEA was included in intracellular solution [11, 75]. 20 mM HEPES was applied to block horizontal cell feedback [34, 76] and 20 mM sucrose was added in Ames' solution and 10 mM KCl was added to intracellular solution for control recordings. AMPA and kainite glutamate receptor antagonists, 6-cyano-7-nitroquinoxaline-2,3-dione (CNQX) (15 µM, Tocris) and 2,3-Dioxo-6-nitro-1,2,3,4-tetrahydrobenzo[f]quinoxaline-7-sulfonamide (NBQX) (10 µM, Tocris), were bath applied to block photoreceptor - horizontal cell transmission. To block gap junction, meclofenamic acid (MFA) (50-100 µM, Sigma) was used. Lastly, we used DL-threo-β-Benzyloxyaspartic acid (DL-TBOA, 50 µM, Tocris) to inhibit EAAT5.

Light stimulation

A green (500 nm) spot light was directed through a 60× objective lens to illuminate photoreceptors around the recorded cells using an LED light source (pE-2, Cool LED, UK). The diameter of the spot was approximately 150-200 µm. We defined the scotopic light levels as 10^{-1}-10^{1} photons/ µm^2/s, mesopic light levels between 10^{2}-10^{4} photons/ µm^2/s and photopic range as greater than 10^{5} photons/ µm^2/s. The preparations were adapted to background illumination either dark (for scotopic recording) or at the mesopic range for approximately 10 minutes prior to recording. A step of light (equivalent to 1 log unit step, lasting 1-2 seconds) was projected on top of the background illumination. The light response at each background was checked twice for SAC and bipolar cells recordings: after incrementing backgrounds, we would return to the preceding lower intensity background to check the original response; one-minute intervals were used between backgrounds. For searching and recording the tdTomato-labeled SACs, we briefly (up to several seconds) exposed bright red light (560 nm, pE-2 system, at 10^{8} photons/ µm^2/s) to identify SAC somas in Ai9; ChAT-cre mice.

Morphological Identification

A patch clamp pipette was filled with a fluorescent dye, sulforhodamine B (0.005%, Sigma) or Alexa 488 (0.003%, ThermoFisher Scientific, Waltham, MA). Immediately following electrophysiological recordings, images of bipolar cells were visualized and their morphological

types confirmed by their dendritic characterizations (SAC) and axonal ramification patterns (BC) in the IPL [22]. Images of both axon terminals and ChAT-bands were captured and recorded using a CCD camera.

For some retinal tissues without ChAT-band fluorescence, such as wildtype and *Cnga3*$^{-/-}$, we included Neurobiotin (0.5%, Vector Lab, CA, USA) in the pipette solution along with a fluorescent dye [4, 5]. To visualize cells with Neurobiotin, the preparation was fixed with 4% paraformaldehyde for 30 minutes, then incubated overnight with streptavidin-conjugated Alexa 488 (1:200, Thermo Fisher Scientific) and an anti-choline acetyltransferase (ChAT) antibody (1:200, AB144P, Millipore, MA, USA). Subsequently, the preparation was incubated with the secondary antibody for 2 hours at room temperature. The preparation was then observed using a confocal microscope (TCS SP8, Leica, Germany). Bipolar cell types were identified based on previous descriptions [4, 5, 77]. For ON-SAC recordings, we targeted cells using Ai9-tdTomato mice or blindly in C57 mice, using previously established guidelines for identifying SACs [78, 79].

Data analysis and statistics

For step-pulse light-evoked L-EPSPs, we measured the peak amplitude (in millivolts) from the baseline using Clampfit software (Molecular Devices). All values are presented as the mean ± SEM. Data normality was assessed before statistical testing. SAC and bipolar cell responses to pharmacological agents were evaluated using paired or unpaired *t*-tests and linear mixed-effects models, as appropriate, followed by Holm's multiple comparison correction. Linear mixed-effects models were used to evaluate whether response amplitude changed systematically across light levels (mesopic to photopic), considering cell identity as a random effect to account for repeated measurements across light levels within the same cell, using Wald t-statistics. Bipolar cell polarity switches were evaluated using pared t-tests. Light levels and polarity switches were compared using post-hoc paired pairwise t-tests with Holm's multiple comparison correction. To assess polarity changes, McNemar's tests or Cochran-Armitage trend tests were applied to the binary polarity data (positive vs. negative), with zero amplitude responses excluded. To account for zero amplitudes, Stuart-Maxwell tests were also used for the polarity data with three levels (positive, zero, and negative). All statistical analyses were performed using Prism 10.4 (GraphPad Software Inc., CA) and the statistical software package R (version 4.3.2). Statistical significance was set at $p<0.05$.

Data Availability

Supplementary Data 1 includes all source data and is provided with this paper. Any additional data is available from the corresponding author upon reasonable request.

Acknowledgements

We would like to thank Drs. Dao-Qi Zhang and Samar Hattar for providing photoreceptor KO mice. We also thank Dr. Manoranjan Santra for genotyping support and Mr. Bashir Khatib-Shahidi and Mr. Goichi Suganuma for technical assistance. We are grateful to generous research funding: NIH EY028915 (TI), NIH EY032917 (TI), NIH EY004068 (Vision Core), Rumble Fellowship (JB), and RPB grant.

Author Contributions

C.B.H. and T.I. were responsible for conceptualizing the study. D.L.B., A.R.H., A.S. J.M.B. and C.B.H. performed patch clamp study and analyzed data. D.L.B. and S.K performed statistical analysis. Y.U. and E.C.S. advised on light adaptations and provided photoreceptor mutant mouse analysis. T.I. wrote original manuscript. D.L.B., A.R.H., A.S., and C.B.H. generated figures. All authors reviewed and edited the manuscript.

Competing interests. Authors declare no competing interests.

Materials & Correspondence. Material and correspondence requests should be addressed to the corresponding author, Tomomi Ichinose, MD, PhD.

Figure Legend

Fig. 1

ON and OFF SACs exhibit polarity switch. **a.** An ON SAC labeled with an intracellular fluorescent dye, sulforhodamine b. **b.** A family of whole cell currents in response to 10 mV depolarizing steps from -70 to +20 mV, showing transient outward potassium currents without sodium currents. **c. i**. Three representative depolarizing responses from 3 ON SACs to 1-second step light stimulus (yellow bar) at mesopic conditions. **ii**. Atypical hyperpolarizing light-evoked responses of 3 ON SACs to same stimulus as (**i**). **d.** Three representative traces from 3 OFF SACs recorded with the same conditions as **(c)**. **e.** Comparison of resting membrane potentials (Vm) for the depolarizing vs. hyperpolarizing ON and OFF SACs. Statistical significance was assessed using an unpaired t-test. N= 4 depolarized, and n=13 hyperpolarized ON SACs and n=8 depolarized and n=2 hyperpolarized OFF SACs Error bars, s.e.m, $p>0.05$ for ON and OFFSACS. **f.** Polarities of ON SACs where light responses to spot stimuli were recorded both at the beginning and after more than 10 minutes of recordings. The number of ON SACs exhibits initial depolarizing (ON, white) or hyperpolarizing (OFF, black) responses with progression of responses.

Fig. 2

Polarity switch in ON SACs was not induced by antagonistic surround, nor by OFF signaling crossover. **a.** A hyperpolarizing L-EPSP to a 1-second step light stimulus (yellow) in an ON SAC before (black) and after (red) application of 1 µM strychnine and 50 µM bicuculline to block glycine and GABA-A receptors. A graph summarizes L-EPSP amplitudes from 7 ON SACs, showing no effects on polarity switch. **b.** A hyperpolarizing ON SAC before (black) and after (red) application of 10 µM CGP-52432, a GABA-B antagonist. A graph summarizes L-EPSP amplitudes from 4 ON SACs. **c.** A hyperpolarizing ON SAC before and after application of 50 µM TPMPA, a GABA-C antagonist, in addition to strychnine, bicuculline, and CGP-52432. The white circles represent responses after application of Str, Bic & TPMPA, while the blue squares represent the latter 3 blockers + CGP. A graph summarizes L-EPSP amplitudes from 7 ON SACs. **d.** A hyperpolarizing ON SAC before and after application of 10 µM L-AP4, an mGluR6 agonist, to block mGluR6 signaling. A graph showing L-EPSP amplitudes for three conditions from 8 ON SACs. In all graphs for this and subsequent figures, circles indicate the amplitudes of individual cells and large triangle symbols indicate average of the responses. Paired pairwise t-tests were used for all panels, with Holm's multiple comparison correction applied. Asterisks represent statistically significant effects.

Fig. 3

Increasing luminance levels corrected polarity switch in ON and OFF SACs and CBCs. **a.** An ON SAC exhibited hyperpolarized L-EPSPs at mesopic (Meso.) light levels (yellow bar indicates the timing of light stimulus) and became more depolarized as the background light levels increased to photopic (Phot.) range. In all panels, the black trace is the average of the gray trials. A graph at the bottom showing L-EPSP amplitudes in 11 ON SAC cells from mesopic to photopic luminance. Black circles indicate response amplitude in individual ON SAC, and green

triangles show average responses. Four light levels from Meso. to Phot. were 10^3, 10^4, 10^5, and 10^6 photons/μm^2/s for both panels and summary graphs. **b.** An OFF SAC depolarized at the light onset in the mesopic conditions and became more hyperpolarized as the background light levels increased to photopic. A graph at the bottom showing 8 OFF SACs exhibiting similar responses (black circles show individual OFF SACs, and magenta triangles show average responses). **c.** An ON CBC exhibited hyperpolarizing L-EPSP at mesopic levels, which became more depolarized as the background light levels increased to photopic. A graph at the bottom showing 9 ON CBCs with similar progression over increase in luminance levels. **d.** An OFF CBC exhibited depolarizing L-EPSP in mesopic conditions became more hyperpolarized as background light levels increased to photopic. A graph at the bottom shows 2 OFF bipolar cells with similar progression over increase in luminance levels. **e.** Resting membrane potentials for the 4 cell types and luminance conditions. All statistical tests in this figure were performed using linear mixed-effects models. Linear mixed-effects models were used to evaluate whether response amplitude changed systematically across light levels (mesopic to photopic), considering cell identity as a random effect to account for repeated measurements across light levels within the same cell, using Wald t-statistics. Asterisks represent statistically significant effects.

Fig. 4

Rod and cone dysfunctional mutant mice and polarity switch. **a.** (*left*) L-EPSPs were recorded from an ON CBC in response to 1 log step stimulus (yellow bar) in *Gnat1*$^{-/-}$ at mesopic and photopic background luminances. This cell showed no response at mesopic and depolarized at the photopic background level, exhibiting no polarity switch. (*right*) L-EPSPs were recorded from an OFF CBC, showed no response at mesopic and hyperpolarized at the photopic light level, showing no polarity switch. A summary graph for peak amplitudes of L-EPSPs for ON CBCs (**i**) and OFF CBCs (**ii**) showed no response in mesopic but responded with a correct polarity in photopic. Here and in subsequent panels, black circles indicate peak amplitudes in individual CBCs, and green (ON CBCs, n=5, p<0.05) and magenta (OFF CBCs, n=5, p<0.05) triangles show average responses. **b.** Representative L-EPSPs in ON and OFF CBCs in *Cnga3*$^{-/-}$ at mesopic and photopic conditions in response to 1 log step stimulus (yellow bar). Polarity switch was observed in mesopic and correct polarity L-EPSPs were evoked in photopic conditions. The black trace is the average of the gray trials for all examples. **i.** A graph showing peak amplitudes for 10 ON CBCs at mesopic and photopic conditions (n=10, p<0.005). **ii**. OFF CBCs for same conditions as (**i**) (n=10, p<0.005). **c.** Representative L-EPSPs for an ON and OFF CBCs in *Gnat2*$^{-/-}$ cone dysfunctional mice. **i.** Peak amplitudes for ON CBCs, which showed a polarity switch in mesopic and correct polarity in photopic (black circles) (n=8, p<0.005). **ii.** Peak amplitudes for OFF CBCs for same conditions as (**i**) (n=10, p<0.005). All statistical tests in this figure were performed using paired *t*-tests followed by Holm's multiple comparison correction. Asterisks represent statistically significant effects.

Fig. 5

Gap junctions mediated correct polarity but not polarity switch in ON and OFF CBCs. **a.** L-EPSPs in an OFF CBC in WT retina in response to 1 log unit step light (yellow bar) at mesopic

background luminance before and during application of 100 μM MFA to block gap junctions. The black trace is the average of the gray individual traces for the condition. (*left*) L-EPSPs exhibited polarity switch in control, which was not changed as the drug took effect. (*right*) L-EPSPs in photopic background luminance. The hyperpolarizing L-EPSP was converted to depolarization as the drug took effect. **b.** (*upper*) A summary graph shows L-EPSP amplitudes from ON CBCs in two different background levels and before and after the MFA application (n=3, $p<0.05$). One ON cell did not show polarity switch initially, but the response was flipped after MFA. (*lower*) OFF CBCs showed similar results to the upper panel (n=4, $p<0.05$). **c.** An ON CBC recorded in a *Cx36-fl/fl;Rho-Cre* retina shows a switched polarity in mesopic conditions and correct polarity at photopic. **d.** A summary graph shows L-EPSP amplitudes for 4 ON and 2 OFF CBCs recorded in *Cx36-fl/fl;Rho-Cre* retinas at two background levels. All statistical tests in this figure were performed using paired t-tests followed by Holm's multiple comparison correction.

Fig. 6

Blocking transmission from photoreceptors to horizontal cells reduced the correct polarity but did not change polarity switch. **a.** L-EPSPs were recorded from an ON CBC in *WT* retina in response to 1 log unit step light for 1 second (yellow bar) in mesopic and photopic conditions and before, during, and after application of 10 μM NBQX, a potent AMPA receptor antagonist. The polarity switch response (hyperpolarization) at mesopic was not converted by NBQX, but correct polarity signal (depolarization) at photopic was flipped to depolarizing after NBQX application. 4 ON cells (3 cells had the polarity switch at the photopic level "black circles", and 1 cell had the polarity switch at the mesopic level "cyan square") and 2 OFF cells showed polarity switch at the photopic level (ON, n=3, $p<0.05$; OFF, n=2, $p<0.05$). **b.** L-EPSPs were recorded from an ON CBC in *Gnat2*$^{-/-}$ cone KO retina (yellow bar) in mesopic and photopic conditions and before, during, and after application of 15 μM CNQX, an AMPA/kainite receptor antagonist. While CNQX did not change flipped L-EPSP in mesopic, it converted the correct polarity response in photopic to a polarity switch. (*right*) A graph shows L-EPSP amplitudes in 7 ON CBCs (Photopic, $p<0.05$), and from 4 OFF CBCs (Photopic, $p<0.05$). **c.** L-EPSPs from an ON CBC from WT retina with the same stimulus in mesopic and photopic. CNQX did not change the polarity switch but converted correct polarity to polarity switch in photopic conditions. Graphs summarize L-EPSP amplitudes from 2 ON and 3 OFF CBCs, showing a similar effect of CNQX. (OFF photopic, $p<0.05$). All statistical tests in this figure were performed using paired t-tests followed by Holm's multiple comparison correction. Asterisks represent statistically significant effects.

Fig. 7

The EAATs mediated the polarity switch in CBCs, and a schematic model showing the polarity dichotomy pathways. **a.** An ON CBC and an OFF CBC exhibited L-EPSPs with polarity switch. DL-TBOA (50 μM) removed the polarity switch for 4 ON CBCs (**ai.** Control, -5.02 ± 1.0 mV; DL-TBOA, 3.89 ± 1.44 mV) and 2 OFF CBCs (**ai.** Control, 4.98 ± 0.16 mV; DL-TBOA, -7.31 ± 1.07 mV) . **aii.** Responses normalized to the maximum absolute switched polarization before DL-TBOA was applied (n=6 CBCS, $p<0.05$) **b.** L-EPSPs without polarity switch in an ON CBC and

an OFF CBC were not changed by DL-TBOA. Similar results were seen in 3 ON CBCs (**bi.** Control, 6.32 ± 0.69 mV; DL-TBOA, 4.46 ± 1.85 mV) and 3 OFF CBCs (**bi.** Control, -5.37 ± 1.32 mV; DL-TBOA, -4.97 ± 2.22 mV) **bii** Responses normalized to the maximum absolute correct polarization before DL-TBOA was applied (n=6 CBCs, p> 0.05. **c.** The resting membrane potential for the control condition vs. DL-TBOA for all CBCs (no significant difference found between ON and OFF Vm, p>0.05). No significant difference was found between the two conditions. (Control, -43.43 ± 1.46 mV; DL-TBOA, -44.21 ± 2.02, n=12 CBCs, p>0.05); **d.** Graphical schematic of a working model for the polarity dichotomy pathways. (1) The correct polarity L-EPSPs (red arrow) originate in rods and cones. Rod-originated signals are mediated through rod-cone coupling and horizontal cells to reach cones. Both rod- and cone-originated signals are then transmitted to ON and OFF CBCs (yellow arrows). (2) The polarity switch signals also originate in rods (blue arrow). Continuously released glutamate activates EAAT5 and Cl- currents in cones in dim light conditions, inhibiting cones. When light stimulus reduces glutamate release from rods, cone inhibition stops, depolarizing the cone terminals. This generates the L-EPSPs with polarity switches in ON and OFF CBCs. Cones are green, rods are dark cyan, horizontal cells are purple, an ON CBC is pink, and an OFF CBC is blue. Paired t-tests followed by Holm's multiple comparison correction were used for panels **a** and **b**, and an unpaired t-test was used for panel **c**.

Table 1

Summary of ON and OFF CBC numbers exhibiting a polarity switch and a correct polarity between mesopic and photopic light conditions for different genetic mouse models. WT = wildtype, RKO = rod knockout, CKO = cone knockout, UK type = unknown type.

References

1. Famiglietti, E.V., Jr., Kaneko, A. & Tachibana, M. Neuronal architecture of on and off pathways to ganglion cells in carp retina. *Science* **198**, 1267-1269 (1977).
2. Famiglietti, E.V., Jr. & Kolb, H. Structural basis for ON-and OFF-center responses in retinal ganglion cells. *Science* **194**, 193-195 (1976).
3. Wu, S.M., Gao, F. & Maple, B.R. Functional architecture of synapses in the inner retina: segregation of visual signals by stratification of bipolar cell axon terminals. *J Neurosci* **20**, 4462-4470 (2000).
4. Ichinose, T., Fyk-Kolodziej, B. & Cohn, J. Roles of ON cone bipolar cell subtypes in temporal coding in the mouse retina. *J Neurosci* **34**, 8761-8771 (2014).
5. Ichinose, T. & Hellmer, C.B. Differential signalling and glutamate receptor compositions in the OFF bipolar cell types in the mouse retina. *J Physiol* **594**, 883-894 (2016).
6. Baden, T.*, et al.* The functional diversity of retinal ganglion cells in the mouse. *Nature* **529**, 345-350 (2016).
7. Baden, T., Berens, P., Bethge, M. & Euler, T. Spikes in mammalian bipolar cells support temporal layering of the inner retina. *Curr Biol* **23**, 48-52 (2013).
8. Borghuis, B.G., Marvin, J.S., Looger, L.L. & Demb, J.B. Two-photon imaging of nonlinear glutamate release dynamics at bipolar cell synapses in the mouse retina. *J Neurosci* **33**, 10972-10985 (2013).
9. Szikra, T.*, et al.* Rods in daylight act as relay cells for cone-driven horizontal cell-mediated surround inhibition. *Nat Neurosci* **17**, 1728-1735 (2014).
10. Vlasits, A.L.*, et al.* A Role for Synaptic Input Distribution in a Dendritic Computation of Motion Direction in the Retina. *Neuron* **89**, 1317-1330 (2016).
11. Ozaita, A.*, et al.* A unique role for Kv3 voltage-gated potassium channels in starburst amacrine cell signaling in mouse retina. *J Neurosci* **24**, 7335-7343 (2004).
12. Perez De Sevilla Muller, L., Shelley, J. & Weiler, R. Displaced amacrine cells of the mouse retina. *J Comp Neurol* **505**, 177-189 (2007).
13. Vlasits, A.L.*, et al.* Visual stimulation switches the polarity of excitatory input to starburst amacrine cells. *Neuron* **83**, 1172-1184 (2014).
14. Zhou, Z.J. & Fain, G.L. Neurotransmitter receptors of starburst amacrine cells in rabbit retinal slices. *J Neurosci* **15**, 5334-5345 (1995).
15. Wassle, H.*, et al.* Glycinergic transmission in the Mammalian retina. *Front Mol Neurosci* **2**, 6 (2009).
16. Jain, V.*, et al.* Gain control by sparse, ultra-slow glycinergic synapses. *Cell Rep* **38**, 110410 (2022).
17. Grzywacz, N.M. & Zucker, C.L. Modeling Starburst cells' GABA(B) receptors and their putative role in motion sensitivity. *Biophys J* **91**, 473-486 (2006).
18. Lukasiewicz, P.D., Maple, B.R. & Werblin, F.S. A novel GABA receptor on bipolar cell terminals in the tiger salamander retina. *J Neurosci* **14**, 1202-1212 (1994).
19. Slaughter, M.M. & Miller, R.F. An excitatory amino acid antagonist blocks cone input to sign-conserving second-order retinal neurons. *Science* **219**, 1230-1232 (1983).
20. Davenport, C.M., Detwiler, P.B. & Dacey, D.M. Effects of pH buffering on horizontal and ganglion cell light responses in primate retina: evidence for the proton hypothesis of surround formation. *J Neurosci* **28**, 456-464 (2008).
21. Bohl, J.M., Shehu, A., Hellmer, C.B. & Ichinose, T. Patch clamp recording from bipolar cells in the wholemount mouse retina. *STAR Protoc* **3**, 101482 (2022).
22. Hellmer, C.B.*, et al.* Cholinergic feedback to bipolar cells contributes to motion detection in the mouse retina. *Cell Rep* **37**, 110106 (2021).

23. Pasquale, R., Umino, Y. & Solessio, E. Rod Photoreceptors Signal Fast Changes in Daylight Levels Using a Cx36-Independent Retinal Pathway in Mouse. *J Neurosci* **40**, 796-810 (2020).
24. Calvert, P.D.*, et al.* Membrane protein diffusion sets the speed of rod phototransduction. *Nature* **411**, 90-94 (2001).
25. Hirano, A.A., Hack, I., Wassle, H. & Duvoisin, R.M. Cloning and immunocytochemical localization of a cyclic nucleotide-gated channel alpha-subunit to all cone photoreceptors in the mouse retina. *J Comp Neurol* **421**, 80-94 (2000).
26. Seeliger, M.W.*, et al.* New views on RPE65 deficiency: the rod system is the source of vision in a mouse model of Leber congenital amaurosis. *Nat Genet* **29**, 70-74 (2001).
27. Ronning, K.E.*, et al.* Loss of cone function without degeneration in a novel Gnat2 knock-out mouse. *Experimental eye research* **171**, 111-118 (2018).
28. Ishibashi, M.*, et al.* Analysis of rod/cone gap junctions from the reconstruction of mouse photoreceptor terminals. *Elife* **11** (2022).
29. Thoreson, W.B., Sladek, A.L., Barta, C.L. & Townsend, L.E. Rod Inputs Arrive at Horizontal Cell Somas in Mouse Retina Solely via Rod-Cone Coupling. *eNeuro* **12** (2025).
30. Mills, S.L. & Massey, S.C. A series of biotinylated tracers distinguishes three types of gap junction in retina. *J Neurosci* **20**, 8629-8636 (2000).
31. Xin, D. & Bloomfield, S.A. Dark- and light-induced changes in coupling between horizontal cells in mammalian retina. *J Comp Neurol* **405**, 75-87 (1999).
32. Peichl, L. & Gonzalez-Soriano, J. Morphological types of horizontal cell in rodent retinae: a comparison of rat, mouse, gerbil, and guinea pig. *Vis Neurosci* **11**, 501-517 (1994).
33. Kamermans, M.*, et al.* Hemichannel-mediated inhibition in the outer retina. *Science* **292**, 1178-1180 (2001).
34. Hirasawa, H. & Kaneko, A. pH changes in the invaginating synaptic cleft mediate feedback from horizontal cells to cone photoreceptors by modulating Ca2+ channels. *J Gen Physiol* **122**, 657-671 (2003).
35. Vessey, J.P.*, et al.* Proton-mediated feedback inhibition of presynaptic calcium channels at the cone photoreceptor synapse. *J Neurosci* **25**, 4108-4117 (2005).
36. Warren, T.J., Van Hook, M.J., Supuran, C.T. & Thoreson, W.B. Sources of protons and a role for bicarbonate in inhibitory feedback from horizontal cells to cones in Ambystoma tigrinum retina. *J Physiol* **594**, 6661-6677 (2016).
37. Chaffiol, A., Ishii, M., Cao, Y. & Mangel, S.C. Dopamine Regulation of GABAA Receptors Contributes to Light/Dark Modulation of the ON-Cone Bipolar Cell Receptive Field Surround in the Retina. *Curr Biol* **27**, 2600-2609 e2604 (2017).
38. Jackman, S.L., Babai, N., Chambers, J.J., Thoreson, W.B. & Kramer, R.H. A positive feedback synapse from retinal horizontal cells to cone photoreceptors. *PLoS Biol* **9**, e1001057 (2011).
39. Nelson, R., Bender, A.M. & Connaughton, V.P. Stimulation of sodium pump restores membrane potential to neurons excited by glutamate in zebrafish distal retina. *J Physiol* **549**, 787-800 (2003).
40. Yang, J.H., Maple, B., Gao, F., Maguire, G. & Wu, S.M. Postsynaptic responses of horizontal cells in the tiger salamander retina are mediated by AMPA-preferring receptors. *Brain Res* **797**, 125-134 (1998).
41. Puller, C., Ivanova, E., Euler, T., Haverkamp, S. & Schubert, T. OFF bipolar cells express distinct types of dendritic glutamate receptors in the mouse retina. *Neuroscience* **243**, 136-148 (2013).
42. Wersinger, E.*, et al.* The glutamate transporter EAAT5 works as a presynaptic receptor in mouse rod bipolar cells. *J Physiol* **577**, 221-234 (2006).
43. Lukasiewicz, P.D., Bligard, G.W. & DeBrecht, J.D. EAAT5 glutamate transporter-mediated inhibition in the vertebrate retina. *Frontiers in Cell Neuroscience* **15**, 1-5 (2021).
44. Hasegawa, J., Obara, T., Tanaka, K. & Tachibana, M. High-density presynaptic transporters are required for glutamate removal from the first visual synapse. *Neuron* **50**, 63-74 (2006).

45. Veruki, M.L., Morkve, S.H. & Hartveit, E. Activation of a presynaptic glutamate transporter regulates synaptic transmission through electrical signaling. *Nat Neurosci* **9**, 1388-1396 (2006).
46. Ichinose, T. & Lukasiewicz, P.D. The mode of retinal presynaptic inhibition switches with light intensity. *J Neurosci* **32**, 4360-4371 (2012).
47. Arriza, J.L., Eliasof, S., Kavanaugh, M.P. & Amara, S.G. Excitatory amino acid transporter 5, a retinal glutamate transporter coupled to a chloride conductance. *Proc Natl Acad Sci U S A* **94**, 4155-4160 (1997).
48. Borghuis, B.G., Looger, L.L., Tomita, S. & Demb, J.B. Kainate receptors mediate signaling in both transient and sustained OFF bipolar cell pathways in mouse retina. *J Neurosci* **34**, 6128-6139 (2014).
49. Pearring, J.N.*, et al.* A role for nyctalopin, a small leucine-rich repeat protein, in localizing the TRP melastatin 1 channel to retinal depolarizing bipolar cell dendrites. *J Neurosci* **31**, 10060-10066 (2011).
50. Morgans, C.W.*, et al.* TRPM1 is required for the depolarizing light response in retinal ON-bipolar cells. *Proc Natl Acad Sci U S A* **106**, 19174-19178 (2009).
51. Koike, C.*, et al.* TRPM1 is a component of the retinal ON bipolar cell transduction channel in the mGluR6 cascade. *Proc Natl Acad Sci U S A* (2009).
52. Euler, T., Haverkamp, S., Schubert, T. & Baden, T. Retinal bipolar cells: elementary building blocks of vision. *Nat Rev Neurosci* **15**, 507-519 (2014).
53. Pang, J.J., Gao, F. & Wu, S.M. Light-evoked excitatory and inhibitory synaptic inputs to ON and OFF alpha ganglion cells in the mouse retina. *J Neurosci* **23**, 6063-6073 (2003).
54. Ichinose, T. & Habib, S. ON and OFF Signaling Pathways in the Retina and the Visual System. *Front Ophthalmol (Lausanne)* **2** (2022).
55. Pearson, J.T. & Kerschensteiner, D. Ambient illumination switches contrast preference of specific retinal processing streams. *J Neurophysiol* **114**, 540-550 (2015).
56. Tikidji-Hamburyan, A.*, et al.* Retinal output changes qualitatively with every change in ambient illuminance. *Nat Neurosci* **18**, 66-74 (2015).
57. Rivlin-Etzion, M., Wei, W. & Feller, M.B. Visual stimulation reverses the directional preference of direction-selective retinal ganglion cells. *Neuron* **76**, 518-525 (2012).
58. Ankri, L., Ezra-Tsur, E., Maimon, S.R., Kaushansky, N. & Rivlin-Etzion, M. Antagonistic Center-Surround Mechanisms for Direction Selectivity in the Retina. *Cell Rep* **31**, 107608 (2020).
59. Jin, N.*, et al.* Genetic elimination of rod/cone coupling reveals the contribution of the secondary rod pathway to the retinal output. *Sci Adv* **8**, eabm4491 (2022).
60. Behrens, C.*, et al.* Retinal horizontal cells use different synaptic sites for global feedforward and local feedback signaling. *Curr Biol* **32**, 545-558 e545 (2022).
61. Lukasiewicz, P.D., Bligard, G.W. & DeBrecht, J. EAAT5 glutamate transporter-mediated inhibition in the vertebrate retina. *Frontiers in Cellular Neuroscience* **15**, 1-6 (2021).
62. Szmajda, B.A. & Devries, S.H. Glutamate spillover between mammalian cone photoreceptors. *J Neurosci* **31**, 13431-13441 (2011).
63. Thoreson, W.B. & Chhunchha, B. EAAT5 glutamate transporter rapidly binds glutamate with micromolar affinity in mouse rods. *J Gen Physiol* **155** (2023).
64. Ingram, N.T., Sampath, A.P. & Fain, G.L. Voltage-clamp recordings of light responses from wild-type and mutant mouse cone photoreceptors. *J Gen Physiol* **151**, 1287-1299 (2019).
65. Vroman, R. & Kamermans, M. Feedback-induced glutamate spillover enhances negative feedback from horizontal cells to cones. *J Physiol* **593**, 2927-2940 (2015).
66. Wong, K.Y., Cohen, E.D. & Dowling, J.E. Retinal bipolar cell input mechanisms in giant danio. II. Patch-clamp analysis of on bipolar cells. *J Neurophysiol* **93**, 94-107 (2005).
67. Tse, D.Y., Chung, I. & Wu, S.M. Possible roles of glutamate transporter EAAT5 in mouse cone depolarizing bipolar cell light responses. *Vision Res* **103**, 63-74 (2014).

68. Makino, C.L.*, et al.* Recoverin regulates light-dependent phosphodiesterase activity in retinal rods. *J Gen Physiol* **123**, 729-741 (2004).
69. Hurley, J.B. & Chen, J. Evaluation of the contributions of recoverin and GCAPs to rod photoreceptor light adaptation and recovery to the dark state. *Prog Brain Res* **131**, 395-405 (2001).
70. Yin, L., Smith, R.G., Sterling, P. & Brainard, D.H. Chromatic properties of horizontal and ganglion cell responses follow a dual gradient in cone opsin expression. *J Neurosci* **26**, 12351-12361 (2006).
71. Tikidji-Hamburyan, A.*, et al.* Rods progressively escape saturation to drive visual responses in daylight conditions. *Nature communications* **8**, 1813 (2017).
72. Frederiksen, R.*, et al.* Rod Photoreceptors Avoid Saturation in Bright Light by the Movement of the G Protein Transducin. *J Neurosci* **41**, 3320-3330 (2021).
73. Calvert, P.D.*, et al.* Phototransduction in transgenic mice after targeted deletion of the rod transducin alpha -subunit. *Proc Natl Acad Sci U S A* **97**, 13913-13918 (2000).
74. Jin, N.*, et al.* Molecular and functional architecture of the mouse photoreceptor network. *Sci Adv* **6**, eaba7232 (2020).
75. Kuznetsov, K.I., Grygorov, O.O., Maslov, V.Y., Veselovsky, N.S. & Fedulova, S.A. Kv3 channels modulate calcium signals induced by fast firing patterns in the rat retinal ganglion cells. *Cell Calcium* **52**, 405-411 (2012).
76. Babai, N. & Thoreson, W.B. Horizontal cell feedback regulates calcium currents and intracellular calcium levels in rod photoreceptors of salamander and mouse retina. *J Physiol* **587**, 2353-2364 (2009).
77. Ghosh, K.K., Bujan, S., Haverkamp, S., Feigenspan, A. & Wassle, H. Types of bipolar cells in the mouse retina. *J Comp Neurol* **469**, 70-82 (2004).
78. Tu, H.Y., Hsu, C.C., Chen, Y.J. & Chen, C.K. Patch Clamp Recording of Starburst Amacrine Cells in a Flat-mount Preparation of Deafferentated Mouse Retina. *Journal of visualized experiments : JoVE* (2016).
79. Zhou, Z.J. Direct Participation of Starburst Amacrine Cells in Spontaneous Rhythmic Activities in the Developing Mammalian Retina. *The Journal of Neuroscience* **18**, 4155 (1998).

Table 1

	Bipolar type	**Polarity switch**		**Non-switch**	
WT	ON	13	Type 5: (5) Type 6/7: (8)	7	Type 7: (1) Type 5: (1) Type 6/7: (2) UK Type: (3)
	OFF	11	Type 3/4: (9) UK Type: (2)	15	Type 1/2: (6) Type 3/4: (7) UK Type: (2)
RKO (*Gnat1*$^{-/-}$)	ON	0		5	Type 5: (3) Type 6: (1) UK Type: (1)
	OFF	0		5	Type 1/2: 1 Type 3: 1 UK Type: 3
CKO (*Cnga3*$^{-/-}$)	ON	10	Type 5: (2) Type 6/7: (2) UK Type: (6)	3	Type 5: (1) Type 6/7: (1) UK Type: (1)
	OFF	10	Type 1/2: (1) Type 3/4: (1) UK Type: (8)	3	UK Type: (3)
CKO (*Gnat2*$^{-/-}$)	ON	8	Type 5: (4) Type 6/7: (1) UK Type: (3)	0	
	OFF	10	Type 1/2: (1) Type 3/4: (3) UK Type: (6)	3	Type 1/2: (1) Type 3/4: (2)

Editorial Summary:

Rod and cone signaling interactions via glutamate spillover are identified as mechanisms underlying ON and OFF light response polarity switches in retinal interneurons.

Peer Review Information:

Communications Biology thanks Takeshi Yoshimatsu and the other, anonymous, reviewer(s) for their contribution to the peer review of this work. Primary Handling Editor: Benjamin Bessieres. A peer review file is available.

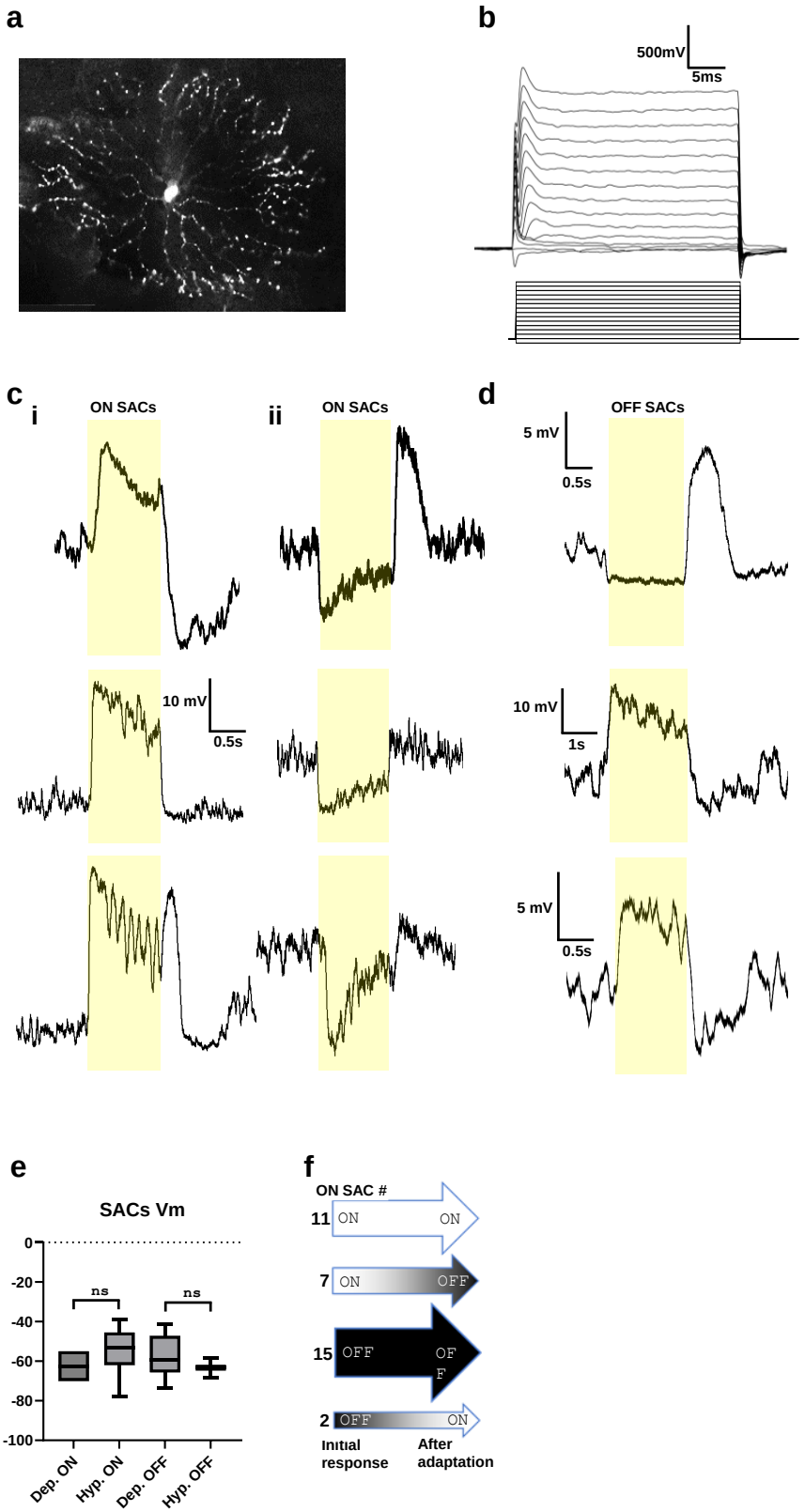
a
b
500mV
5ms
c
i
ON SACs
ii
ON SACs
10 mV
0.5s
d
OFF SACs
5 mV
0.5s
10 mV
1s
5 mV
0.5s
e
SACs Vm
Resting Vm (mV)
0
-20
-40
-60
-80
-100
ns
ns
Dep. ON
Hyp. ON
Dep. OFF
Hyp. OFF
f
ON SAC #
11
ON
ON
7
ON
OFF
15
OFF
OFF
2
OFF
ON
Initial response
After adaptation

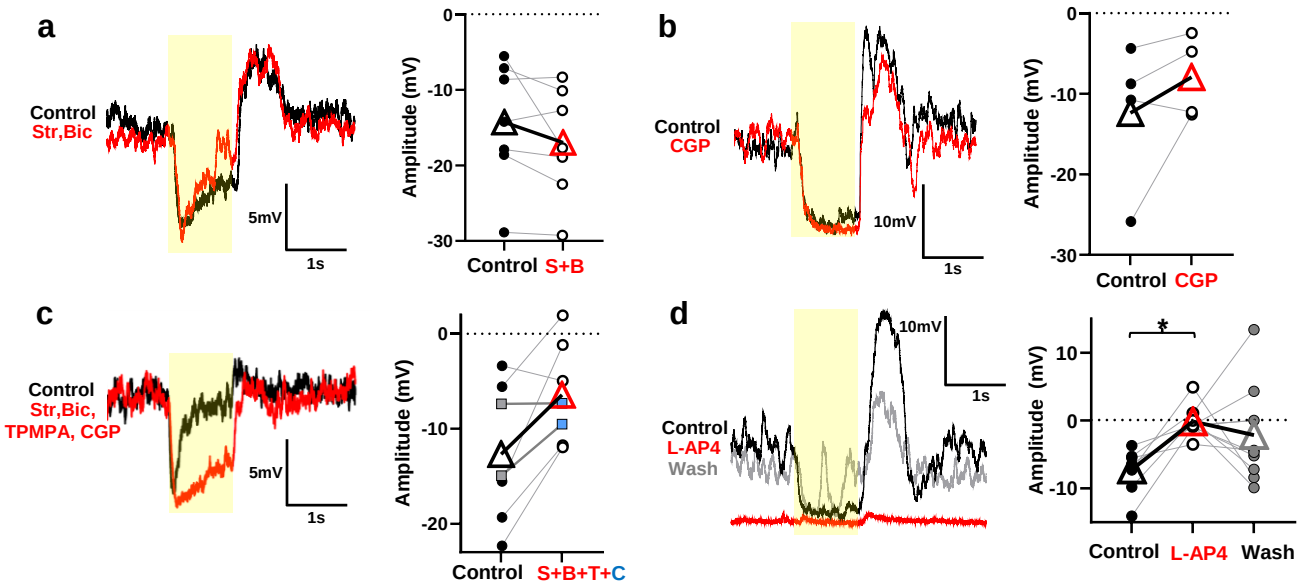
a
Control
Str,Bic
5mV
1s
Amplitude (mV)
0
-10
-20
-30
Control
S+B
b
Control
CGP
10mV
1s
Amplitude (mV)
0
-10
-20
-30
Control
CGP
c
Control
Str,Bic,
TPMPA, CGP
5mV
1s
Amplitude (mV)
0
-10
-20
Control
S+B+T+C
d
10mV
1s
Control
L-AP4
Wash
*
Amplitude (mV)
10
0
-10
Control
L-AP4
Wash

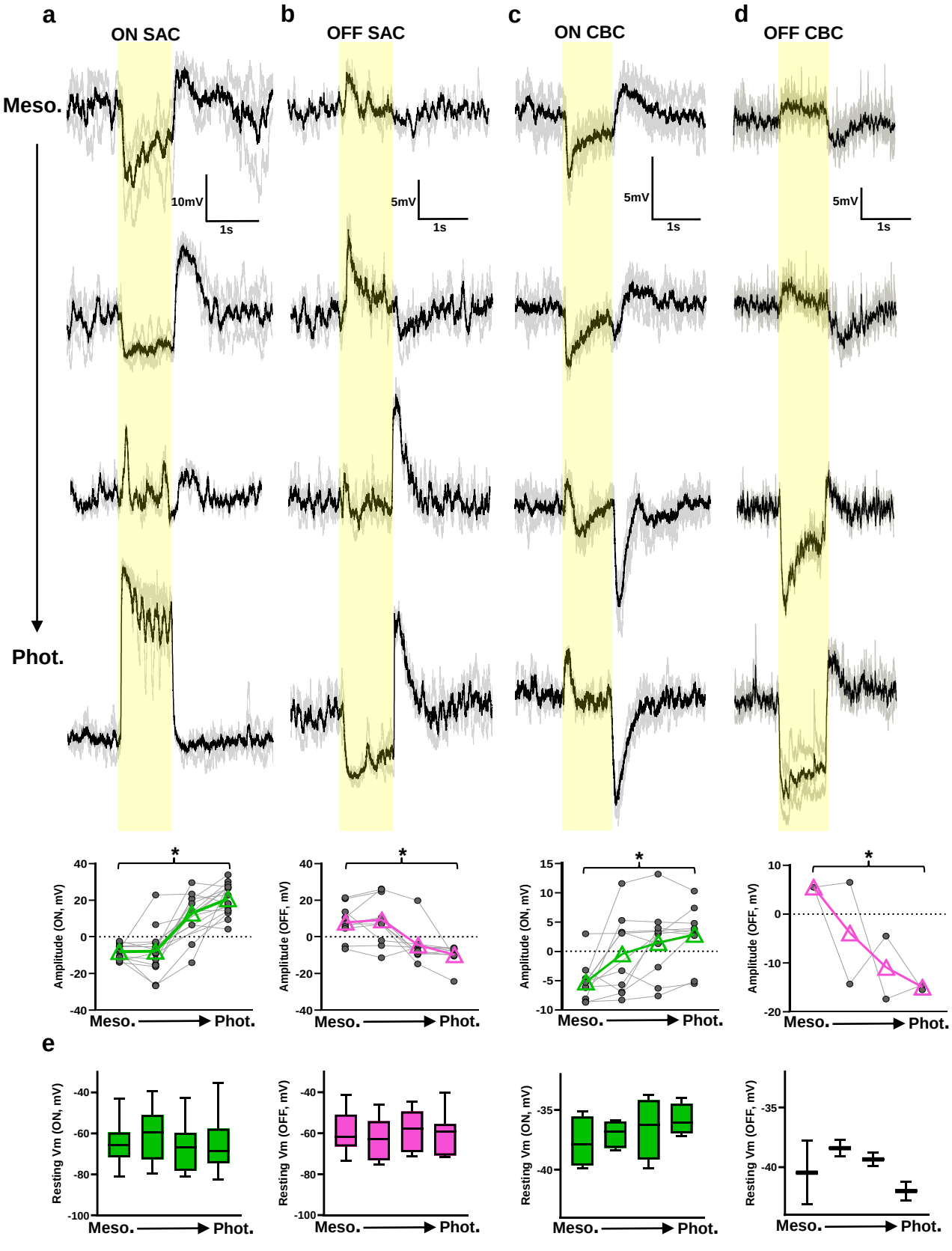
a
ON SAC
b
OFF SAC
c
ON CBC
d
OFF CBC
Meso.
Phot.
10mV
1s
5mV
1s
5mV
1s
5mV
1s
Amplitude (ON, mV)
Amplitude (OFF, mV)
Amplitude (ON, mV)
Amplitude (OFF, mV)
Meso.
Phot.
e
Resting Vm (ON, mV)
Resting Vm (OFF, mV)
Resting Vm (ON, mV)
Resting Vm (OFF, mV)

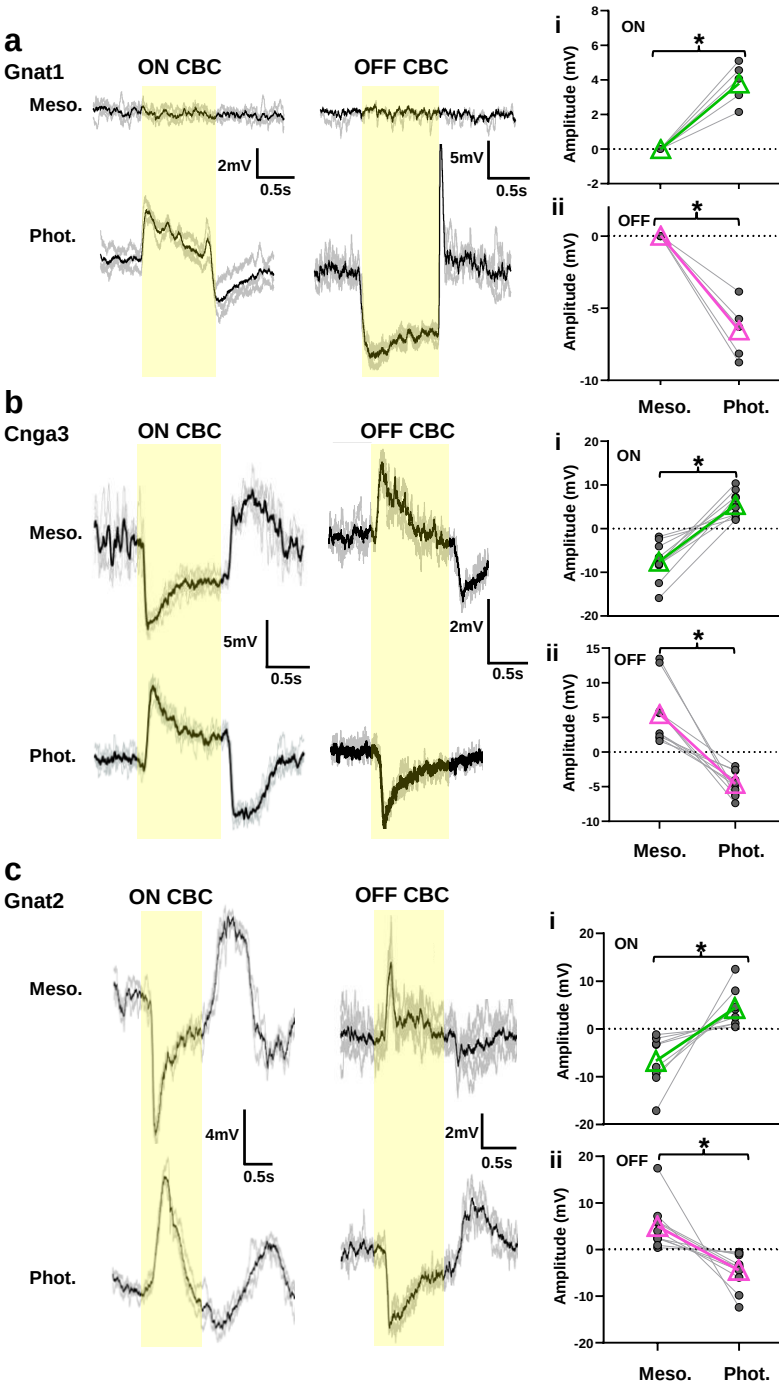
a
Gnat1
ON CBC
OFF CBC
Meso.
Phot.
2mV
0.5s
5mV
0.5s
i
ON
*
Amplitude (mV)
ii
OFF
*
Amplitude (mV)
Meso.
Phot.
b
Cnga3
ON CBC
OFF CBC
Meso.
Phot.
5mV
0.5s
2mV
0.5s
i
ON
*
Amplitude (mV)
ii
OFF
*
Amplitude (mV)
Meso.
Phot.
c
Gnat2
ON CBC
OFF CBC
Meso.
Phot.
4mV
0.5s
2mV
0.5s
i
ON
*
Amplitude (mV)
ii
OFF
*
Amplitude (mV)
Meso.
Phot.

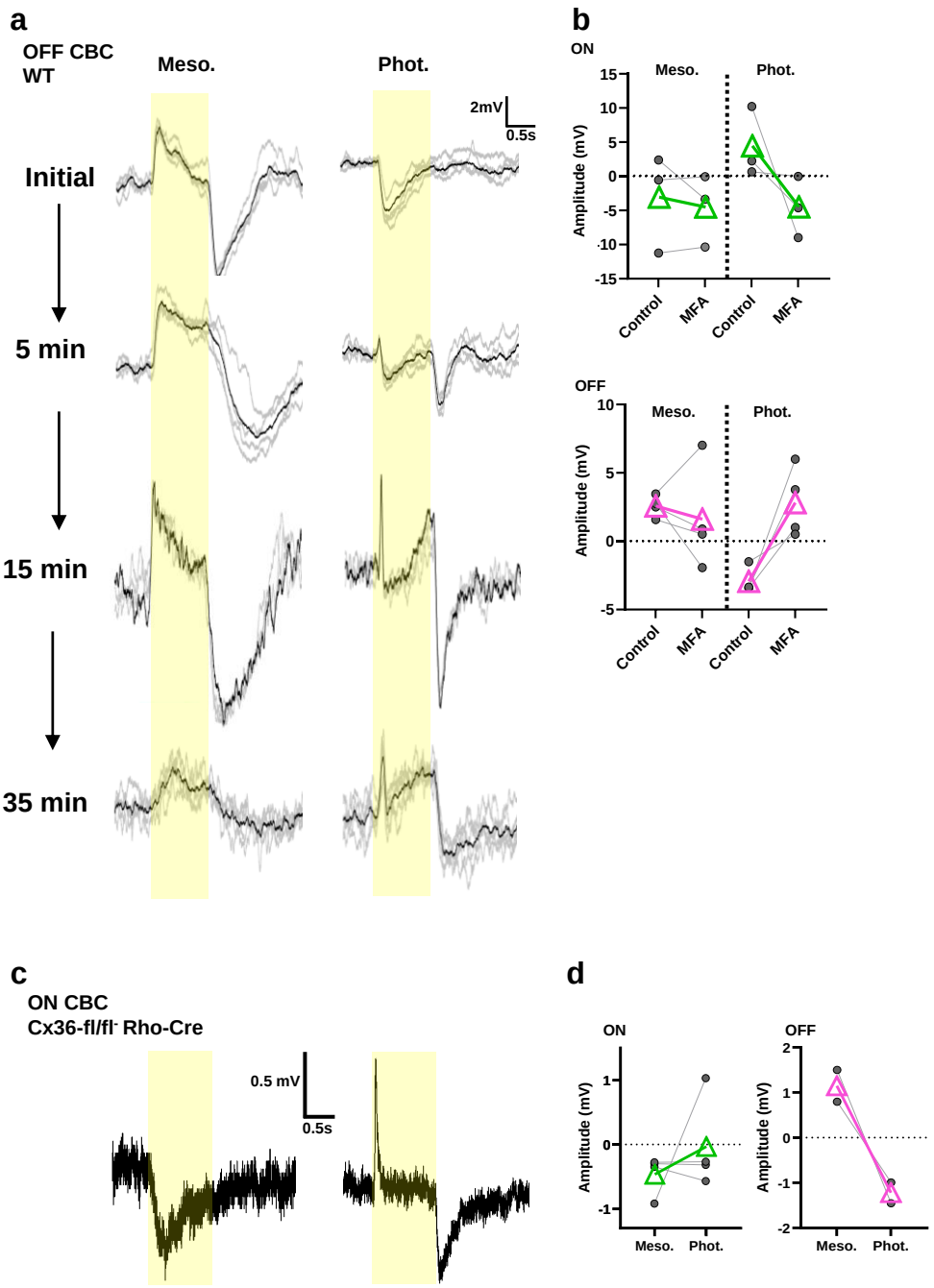
a
OFF CBC
WT
Meso.
Phot.
2mV
0.5s
Initial
5 min
15 min
35 min
b
ON
Meso.
Phot.
Amplitude (mV)
Control
MFA
OFF
c
ON CBC
Cx36-fl/fl- Rho-Cre
0.5 mV
0.5s
d
ON
OFF

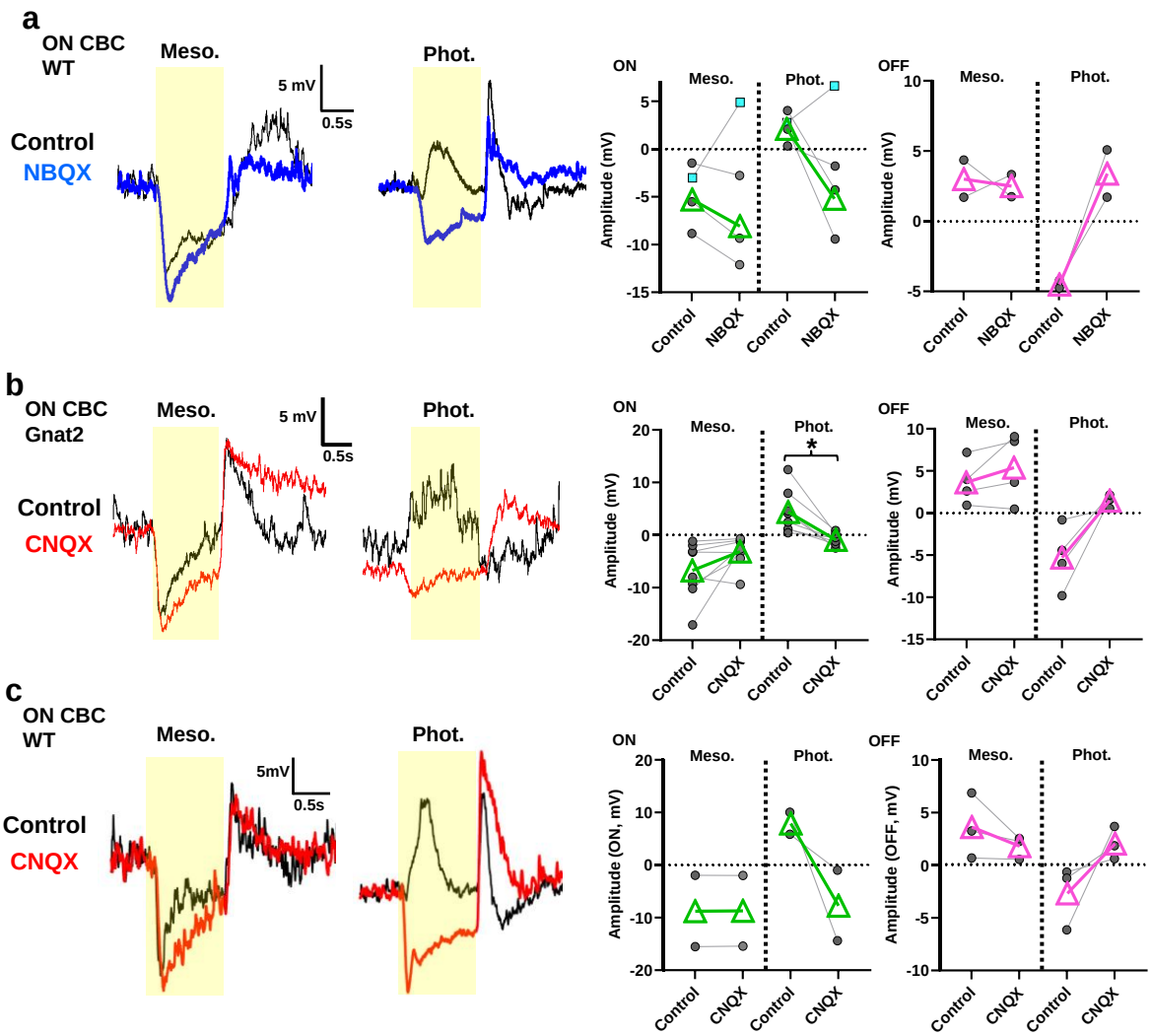
a
ON CBC
WT
Meso.
Phot.
5 mV
0.5s
Control
NBQX
ON
OFF
Amplitude (mV)
Control
NBQX
b
ON CBC
Gnat2
CNQX
*
c
ON CBC
WT
5mV
Amplitude (ON, mV)
Amplitude (OFF, mV)

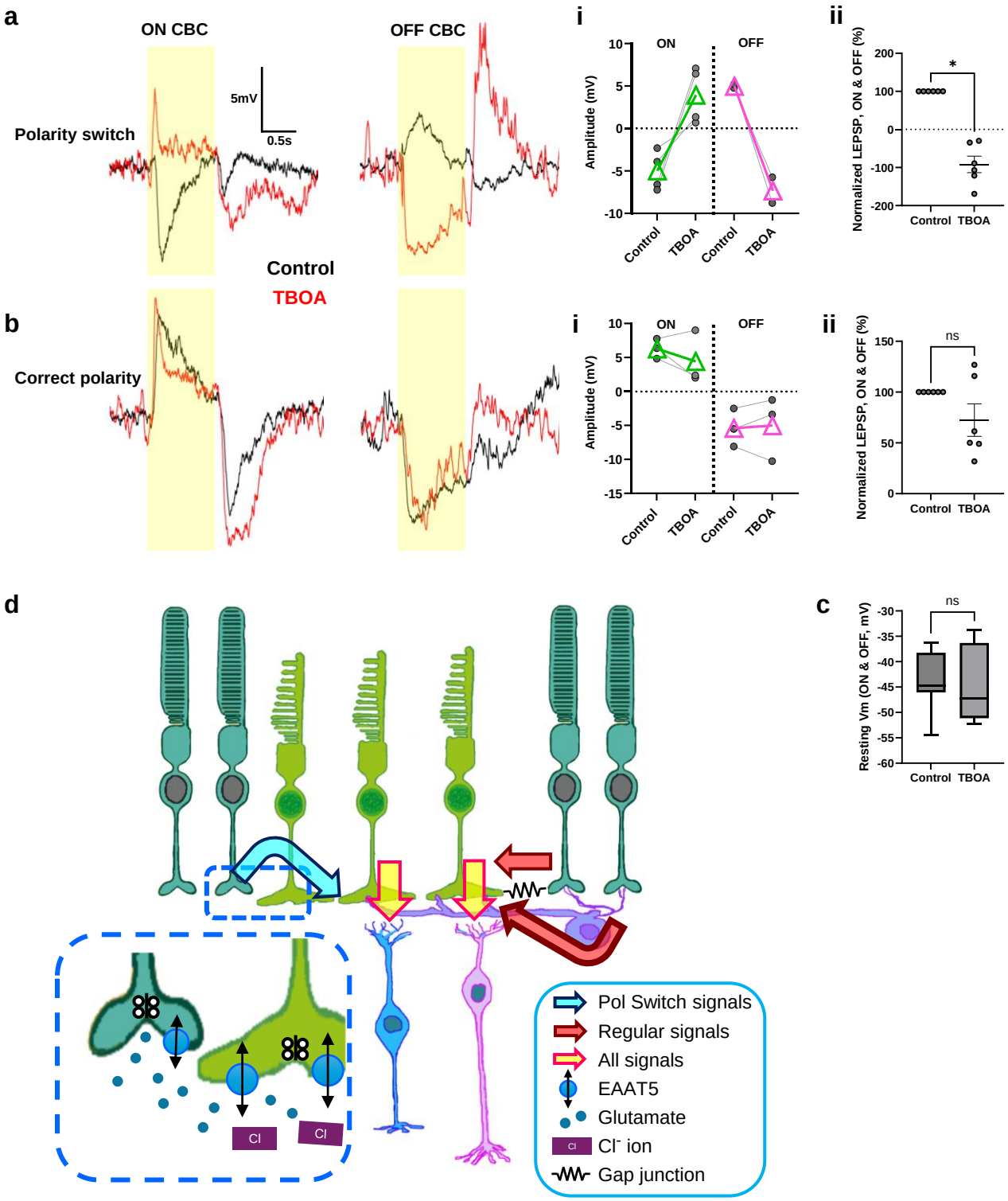
a
ON CBC
OFF CBC
Polarity switch
5mV
0.5s
Control
TBOA
b
Correct polarity
i
ON
OFF
Amplitude (mV)
Control
TBOA
ii
Normalized LEPSP, ON & OFF (%)
*
ns
c
Resting Vm (ON & OFF, mV)
d
Cl
Pol Switch signals
Regular signals
All signals
EAAT5
Glutamate
Cl- ion
Gap junction